Inorganic Chemistry
Article

Inorg. Chem. **2009**, *48*, 10275–10280 **10275**
DOI: 10.1021/ic901416m

$AsMo_7O_{27}$-Bridged Dinuclear Sandwich-Type Heteropolymolybdates of Cr(III) and Fe(III): Magnetism of $[MM'(AsMo_7O_{27})_2]^{12-}$ with MM′ = FeFe, CrFe, and CrCr

Haisheng Xu,[†,§] Lili Li,[†] Bin Liu,[†] Ganglin Xue,*[,†] Huaiming Hu,[†] Feng Fu,[‡] and Jiwu Wang[‡]

[†]*Key Laboratory of Synthetic and Natural Functional Molecule Chemistry (Ministry of Education), Shaanxi Key Laboratory of Physico-Inorganic Chemistry, Department of Chemistry, Northwest University, Xi'an, 710069, China,* [‡]*Shaanxi Key Laboratory of Chemical Reaction Engineering, Yanan University, Yan'an, Shaanxi, China 716000, and* [§]*College of Chemistry and Chemical Engineering, Xi'an Shiyou University, Xi'an, China 710065*

Received July 20, 2009

Two new dinuclear sandwich-type heteropolymolybdates based on the mulitidendate inorganic fragment $[AsMo_7O_{27}]$ and Cr(III) and Fe(III) ions, namely, the homometallic sandwich polyoxometalate (POM) $(NH_4)_{12}[Fe_2(AsMo_7O_{27})_2]\cdot 12H_2O$ (**1**) and the first example of the "symmetrical" heterometallic Cr(III)−Fe(III) sandwich POM, $(NH_4)_{12}$-$[FeCr(AsMo_7O_{27})_2]\cdot 13H_2O$ (**2**), were simultaneously synthesized in high yield. Their magnetic properties are thoroughly investigated together with the homometallic sandwich POM $(NH_4)_{12}[Cr_2(AsMo_7O_{27})_2]\cdot 11H_2O$ (**3**). The $\chi_M T$ values for compounds **1**−**3** at 300 K correspond well to the calculated spin-only values for Fe^{III} ($S = 5/2$) and Cr^{III} (S=3/2) with g_{Fe}= $g_{Cr} = 2$. Upon cooling, the $\chi_M T$ values decline monotonously and reach 0.14, 1.00, and 0.11 $cm^3\ K\ mol^{-1}$ at 2.0 K for **1**, **2**, and **3**, respectively, indicating a significant antiferromagnetic exchange between the magnetic centers with $J = -2.09$, -4.09, and $-6.26\ cm^{-1}$, respectively, for **1**, **2**, and **3**. The magnetic results clearly establish that compound **2** is formed by bimetallic Cr(III)−Fe(III) units and not by a mixture of the two antiferromagnetically coupled homometallic species. Their thermal properties are also characterized.

Introduction

The chemistry of transition-metal-substituted polyoxometalates (TMSPs) has been attracting extensive interest in many different areas of science and technology because of the high versatility of their electronic and structural variation.[1−4] Among the TMSPs, a great subclass is sandwich-type TMSPs composed of diamagnetic vacant fragments and a central transition metal cluster, which have received much attention in recent years. In addition to the traditional interest in catalysis, such species are of particular interest in magnetism because they can provide ideal examples to study magnetic interactions with different exchange-coupled centers on a molecular orbital basis.[5−12] To date, the Weakley-, Hervé-, Krebs-, and Knoth-type and other types of sandwich structures have been reported.[8−13] The great advantage of these complexes is the possibility of varying either the type of the metallic cluster (its topology and the nature of the transition metals) or the heteroatom. All of the above-mentioned POMs are polyoxotungstates with two or more than two paramagnetic metal centers; however, sandwich-type polymolybdates are scarce because of the structural lability of lacunary heteropolymolybdate in aqueous solution, resulting in the difficulty in obtaining a sandwich-type molybdate.[14] Recently, our group reported the structure and preparation of two homometallic sandwich polymolybdates, $[Cr_2(AsMo_7O_{27})_2]^{12-}$ and $[Cu_2(AsMo_7O_{27})_2]^{14-}$,[15] in which two transition metals are sandwiched between two novel $[As(III)Mo_7O_{27}]$ fragments. Interestingly, the distance of two

*To whom correspondence should be addressed. E-mail: xglin707@163.com.

(1) Pope, M. T. *Heteropoly and Isopoly Oxometalates*; Springer-Verlag: Berlin, 1983.
(2) Pope, M. T.; Müller, A. *Polyoxometalates: From Platonic Solids to Anti-RetroViral Activity*; Kluwer: Dordrecht, The Netherlands, 1994.
(3) Pope, M. T.; Müller, A. *Polyoxometalates from Topology via Self-Assembly to Applications*; Kluwer: Dordrecht, The Netherlands, 2001.
(4) Hill, C. L. *Chem. Rev.* **1998**, *98*, 1.
(5) Müller, A.; Peters, F.; Pope, M. T.; Gatteschi, D. *Chem. Rev.* **1998**, *98*, 239.
(6) Ritchie, C.; Ferguson, A.; Nojiri, H.; Miras, H. N.; Song, Y. F.; Long, D. L.; Burkholder, E.; Murrie, M.; Kögerler, P.; Brechin, E. K.; Cronin, L. *Angew. Chem., Int. Ed.* **2008**, *47*, 5609.
(7) Gómez-Garcia, C. J.; Coronado, E.; Gómez-Romero, P.; Casañ-Pastor, N. *Inorg. Chem.* **1993**, *32*, 89.
(8) Botar, B.; Kögerler, P.; Hill, C. L. *Inorg. Chem.* **2007**, *46*, 5398.
(9) Yamase, T.; Abe, H.; Ishikawa, E.; Nojiri, H.; Ohshima, Y. *Inorg. Chem.* **2009**, *48*, 138.
(10) Clemente-Juan, J. M.; Coronado, E.; Gaita-Ariño, A.; Giménez-Saiz, C.; Chaboussant, G.; Güdel, H. U.; Burriel, R.; Mutka, H. *Chemistry* **2002**, *8*, 5701.
(11) Kortz, U.; Jeannin, Y. P.; Tézé, A.; Hervé, G.; Isber, S. *Inorg. Chem.* **1999**, *38*, 3670.
(12) (a) Hay, P. J.; Thibeault, J. C.; Hoffmann, R. *J. Am. Chem. Soc.* **1975**, *97*, 4884. (b) Kahn, O. *Angew. Chem., Int. Ed. Engl.* **1985**, *24*, 834. (c) Kitagawa, S.; Okubo, T.; Kawata, S.; Kondo, M.; Katada, M.; Kobayashi, H. *Inorg. Chem.* **1995**, *34*, 4790. (d) Borrás-Almenar, J. J.; Clemente-Juan, J. M.; Coronado, E.; Tsukerblat, B. S. *Inorg. Chem.* **1999**, *38*, 6081.

Published on Web 10/01/2009

transition metals is about 3.1 Å, which is shorter than the 5 Å of the discrete oxalato-bridged dinuclear complexes thoroughly studied in magnetochemistry,[16] also shorter than the 3.5−3.6 Å of one-μ-O bridged dinuclear complexes,[17] and much shorter than the ca. 10 Å of Krebs-sandwich species.[18] It is well-known that the magnetic coupling can be influenced by the M−O−M′ angle as well as the M···M′ distance. With the aim to clarify the nearest-neighbor exchange interactions occurring in these bimetallic clusters in sandwich POMs, herein, we report the synthesis and structure of the homometallic sandwich POMs $(NH_4)_{12}[Fe_2(AsMo_7O_{27})_2]\cdot 12H_2O$ (**1**) and the first example of the "symmetrical" heterometallic Cr(III)−Fe(III) sandwich POMs, $(NH_4)_{12}[FeCr(AsMo_7O_{27})_2]\cdot 13H_2O$ (**2**). Their magnetic properties are investigated together with the Cr analogue, $(NH_4)_{12}[Cr_2(AsMo_7O_{27})_2]\cdot 11H_2O$ (**3**).[15] The magnetic results clearly establish that **2** is formed by bimetallic Cr(III)−Fe(III) units and not by a mixture of the two antiferromagnetically coupled homometallic species.

Table 1. Summary of Crystallographic Data for the Structures of $(NH_4)_{12}[Fe_2(AsMo_7O_{27})_2]\cdot 12H_2O$ (**1**) and $(NH_4)_{12}[FeCr(AsMo_7O_{27})_2]\cdot 13H_2O$ (**2**)

	1	**2**
empirical formula	$As_2Fe_2H_{72}Mo_{14}N_{12}O_{66}$	$As_2CrFeH_{74}Mo_{14}N_{12}O_{67}$
M, g mol^{-1}	2901.40	2915.56
cryst syst	monoclinic	monoclinic
space group	$P\,2_1/n$	$P\,2_1/n$
a (Å)	11.319(2)	11.342(3)
b (Å)	19.376(3)	19.391(5)
c (Å)	16.301(3)	16.240(3)
β (deg)	91.707(3)	91.830(4)
V, Å^3	3573.5(11)	3570.1(15)
Z	2	2
temp (K)	293(2)	293(2)
d_{calcd}, g cm^{-3}	2.696	2.712
GOF	1.008	0.986
R1[a] ($I > 2\sigma(I)$)	0.0488	0.0510
wR2[b] ($I > 2\sigma(I)$)	0.1515	0.1382
R1[a] (all data)	0.0688	0.0799
wR2[b] (all data)	0.1629	0.1481

[a] $R1 = [\sum|F_o| - |F_c|]/[\sum|F_c|]$. [b] $wR2 = \{[\sum w(F_o^2 - F_c^2)^2]/[\sum w(F_o^2)^2]\}^{1/2}$.

Experimental Section

All chemicals were commercially purchased and used without further purification. Elemental analyses (H and N) were performed on a Perkin-Elmer 2400 CHN elemental analyzer; As, Mo, Fe, and Cr were analyzed on an IRIS Advantage ICP atomic emission spectrometer. IR spectra were recorded in the range of 400−4000 cm^{-1} on an EQUINOX55 FT/IR spectrophotometer using KBr pellets. Thermogravimetry−differential scanning calorimetry (TG-DSC) analyses were performed on a NETZSCH STA 449C TGA instrument in flowing N_2 with a heating rate of 10 °C min^{-1}. Magnetic measurements were performed on a Quantum Design MPMS SQUID magnetometer. The experimental susceptibilities were corrected for the diamagnetism of the constituent atoms (Pascal's tables).[19]

Synthesis. **$(NH_4)_{12}[Fe_2(AsMo_7O_{27})_2]\cdot 12H_2O$ (1).** The synthesis of compound **1** was accomplished by adding a solution of As_2O_3 (0.08 g, 0.4 mmol) dissolved in 6 M hydrochloric acid (6 mL) to a solution of $(NH_4)_6Mo_7O_{24}\cdot 4H_2O$ (0.99 g, 0.8 mmol) dissolved in H_2O (10 mL) with vigorous stirring. The pH value was adjusted to 6.5 by adding $NH_3\cdot H_2O$. Then, 0.22 g of $FeCl_3\cdot 6H_2O$ (0.8 mmol) dissolved in a minimum of water was added, and the solution was heated to 80 °C for 10 min. The mixture was filtered and allowed to cool to ambient temperature. After 1−2 h, yellow crystals were isolated (yield: 0.96 g, 85%, based on Mo). IR for **1**: 3441(s), 3154(s), 1623(m), 1401(s), 912(s), 872(s), 821(m), 782(m), 686(s), 513(w) cm^{-1}. Anal. Calcd (Found) for $As_2Fe_2H_{72}Mo_{14}N_{12}O_{66}$: Mo, 46.3 (47.6); As, 5.16 (5.2); Fe, 3.85 (3.7); H, 2.50 (2.43); N, 5.79 (5.77).

$(NH_4)_{12}[FeCr(AsMo_7O_{27})_2]\cdot 13H_2O$ (2). The synthesis of compound **2** was accomplished by adding a solution of As_2O_3 (0.08 g, 0.4 mmol) dissolved in 6 M hydrochloric acid (6 mL) to a solution of $(NH_4)_6Mo_7O_{24}\cdot 4H_2O$ (0.99 g, 0.8 mmol) dissolved in H_2O (10 mL) with vigorous stirring. The pH value was adjusted to 6.5 by adding $NH_3\cdot H_2O$. Then, 0.11 g of $FeCl_3\cdot 6H_2O$ (0.4 mmol) dissolved in a minimum of water was added, and the solution was heated to 80 °C for 10 min. Then, 0.11 g of $CrCl_3\cdot 6H_2O$ (0.4 mmol) dissolved in a minimum of water was added, and the solution was heated to 90 °C for

(13) Representative examples include the following and references therein: (a) Weakley, T. J. R.; Evans, H. T. j.; Showell, J. S.; Tourné, G. F.; Tourné, C. M. *J. Chem. Soc., Chem. Commun.* **1973**, 139. (b) Finke, R. G.; Droege, M.; Hutchinson, J. R.; Gansow, O. *J. Am. Chem. Soc.* **1981**, *103*, 1587. (c) Finke, R. G.; Droege, M. W. *Inorg. Chem.* **1983**, *22*, 1006. (d) Evans, H. T.; Tourné, C. M.; Tourné, G. F.; Weakley, T. J. R. *J. Chem. Soc., Dalton Trans.* **1986**, 2699. (e) Finke, R. G.; Droege, M. W.; Domaille, P. J. *Inorg. Chem.* **1987**, *26*, 3886. (f) Wasfi, S. H.; Rheingold, A. L.; Kokoszka, G. F.; Goldstein, A. S. *Inorg. Chem.* **1987**, *26*, 2934. (g) Weakley, T. J. R.; Finke, R. G. *Inorg. Chem.* **1990**, *29*, 1235. (h) Gómez-García, C. J.; Coronado, E.; Borrás-Almenar, J. J. *Inorg. Chem.* **1992**, *31*, 1667. (i) Casañ-Pastor, N.; Bas-Serra, J.; Coronado, E.; Pourroy, G.; Baker, L. C. W. *J. Am. Chem. Soc.* **1992**, *114*, 10380. (j) Gómez-García, C. J.; Coronado, E.; Gómez-Romero, P.; Casañ-Pastor, N. *Inorg. Chem.* **1993**, *32*, 3378. (k) Gómez-García, C. J.; Borrás-Almenar, J. J.; Coronado, E.; Ouahab, L. *Inorg. Chem.* **1994**, *33*, 4016. (l) Coronado, E.; Gómez-García, C. J. *Comments Inorg. Chem.* **1995**, *17*, 255. (m) Zhang, X.; Chen, Q.; Duncan, D. C.; Campana, C.; Hill, C. L. *Inorg. Chem.* **1997**, *36*, 4208. (n) Zhang, X.; Chen, Q.; Duncan, D. C.; Lachicotte, R. J.; Hill, C. L. *Inorg. Chem.* **1997**, *36*, 4381. (o) Clemente-Juan, J. M.; Coronado, E.; Galán-Mascarós, J. R.; Gómez-García, C. J. *Inorg. Chem.* **1999**, *38*, 55. (p) Bi, L.-H.; Wang, E.-B.; Peng, J.; Huang, R.-D.; Xu, L.; Hu, C.-W. *Inorg. Chem.* **2000**, *39*, 671. (q) Bi, L.-H.; Huang, R.-D.; Peng, J.; Wang, E.-B.; Wang, Y.-H.; Hu, C.-W. *J. Chem. Soc., Dalton Trans.* **2001**, 121. (r) Laronze, N.; Marrot, J.; Hervé, G. *Inorg. Chem.* **2003**, *42*, 5857. (s) Bi, L.-H.; Kortz, U. *Inorg. Chem.* **2004**, *43*, 7961. (t) Hussain, F.; Reicke, M.; Janowski, V.; de Silva, S.; Futuwi, J.; Kortz, U. *C. R. Chim.* **2005**, *8*, 1045. (u) Zhang, Z.; Li, Y.; Wang, E.; Wang, X.; Qin, C.; An, H. *Inorg. Chem.* **2006**, *45*, 4313. (v) Yamase, T.; Fukaya, K.; Nojiri, H.; Ohshima, Y. *Inorg. Chem.* **2006**, *45*, 7698. (w) Zhao, J. W.; Zhang, J.; Zheng, S. T.; Yang, G. Y. *Inorg. Chem.* **2007**, *46*, 10944. (x) Liu, Y.; Liu, B.; Xue, G.; Hu, H.; Fu, F.; Wang, J. *Dalton Trans.* **2007**, *33*, 3634. (y) Piedra-Garza, L. F.; Dickman, M. H.; Moldovan, O.; Breunig, H. J.; Kortz, U. *Inorg. Chem.* **2009**, *48*, 411.

(14) (a) Fukushima, H. F.; Kobayashi, A.; Sasaki, Y. *Acta Crystallogr.* **1981**, *B37*, 1613. (b) Yang, Y.; Xu, L.; Gang, G.; Li, F.; Qiu, Y.; Qu, X.; Liu, H. *Eur. J. Inorg. Chem.* **2007**, 2500. (c) Yang, Y.; Xu, L.; Gao, G.; Li, F.; Qiu, Y.; Qu, X.; Guo, W. *THEOCHEM* **2008**, *886*, 85.

(15) Li, L.; Shen, Q.; Xue, G.; Xu, H.; Hu, H.; Fu, F.; Wang, J. *Dalton Trans.* **2008**, 5698.

(16) (a) Triki, S.; Bérézovsky, F.; Pala, J. S.; Coronado, E.; Gómez-García, C. J.; Clemente, J. M.; Riou, A.; Molinié, P. *Inorg. Chem.* **2000**, *39*, 3771. (b) Ohba, M.; Tamaki, H.; Matsumoto, N.; Okawa, H. *Inorg. Chem.* **1993**, *32*, 5385.

(17) (a) Min, K. S.; Rhinegold, A. L.; Miller, J. S. *J. Am. Chem. Soc.* **2006**, *128*, 40. (b) Liston, D. J.; Kennedy, B. J.; Murray, K. S.; West, B. O. *Inorg. Chem.* **1985**, *24*, 1561. (c) Bakshi, E. N.; Elliott, R. L.; Murray, K. S.; Nichols, P. J.; West, B. O. *Aust. J. Chem.* **1990**, *43*, 707.

(18) (a) Bösing, M.; Loose, I.; Pohlmann, H.; Krebs, B. *Chem.—Eur. J.* **1997**, *3*, 1232. (b) Bösing, M.; Nöh, A.; Loose, I.; Krebs, B. *J. Am. Chem. Soc.* **1998**, *120*, 7252. (c) Loose, I.; Droste, E.; Bösing, M.; Pohlmann, H.; Dickman, M. H.; Rosu, C.; Pope, M. T.; Krebs, B. *Inorg. Chem.* **1999**, *38*, 2688. (d) Krebs, B.; Droste, E.; Piepenbrink, M.; Vollmer, G. *C. R. Acad. Sci. Paris, Ser. IIc* **2000**, *3*, 205. (e) Kortz, U.; Savelieff, M. G.; Bassil, B. S.; Keita, B.; Nadjo, L. *Inorg. Chem.* **2002**, *41*, 783. (f) Limanski, E. M.; Drewes, D.; Droste, E.; Bohner, R.; Krebs, B. *J. Mol. Struct.* **2003**, *656*, 17. (j) Drewes, D.; Limanski, E. M.; Piepenbrink, M.; Krebs, B. *Z. Anorg. Allg. Chem.* **2004**, *630*, 58.

(19) Kahn, O. *Molecular Magnetism*; VCH Publishers: New York, 1993.

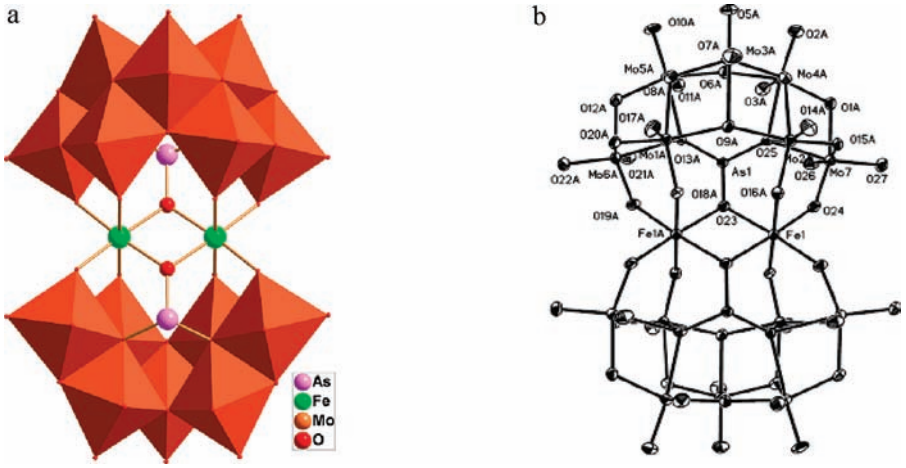

Figure 1. (a) Combined polyhedral/ball-and-stick representation of the polyanion **1a**. (b) ORTEP representation for the structure of **1a**, with displacement ellipsoids shown at 30% probability level.

20 min. The mixture was filtered and allowed to cool to ambient temperature. After 1−2 days, brown crystals were isolated (yield: 0.96 g, 85%, based on Mo). IR for **2**: 3421(s), 3150(s), 1620(m), 1402(s), 900(m), 866(s), 820(m), 788(m), 687(s), 612(m), 511(w) cm^{-1}. Anal. Calcd (Found) for $As_2CrFeH_{74}Mo_{14}N_{12}O_{67}$: Mo, 46.1 (45.6); As, 5.13 (5.3); Fe, 1.91 (1.8); Cr, 1.78 (1.7); H, 2.56 (2.46); N, 5.77 (5.82).

$(NH_4)_{12}[Cr_2(AsMo_7O_{27})_2]\cdot 11H_2O$ (3). Compound **3** was synthesized according to the published procedure.[15]

X-Ray Crystallography. Intensity data were collected on a Rigaku Bruker SMART APEX II CCD diffractometer with Mo Kα monochromated radiation (λ = 0.71073 Å) at 293 K. Empirical absorption correction was applied. The structures of **1** and **2** were solved by the direct method and refined by full-matrix least-squares on F^2 using the SHELXTL-97 software. Heavy atoms (Mo, As, Fe, and Cr) and the framework oxygen atoms of the polyanions were refined with anisotropic displacement parameters; the other oxygen atoms were refined isotropically. Hydrogen atoms were not included. As usual, for most polyoxometalates crystallized with amounts of water, which with the counterions fill the cavities formed by the molecular arrangement, the crystal shows some disorder in the range of counterions and water molecules. For these hydrated ammonium salts, the data did not support discrimination between oxygen and nitrogen atoms, and the ammonium ions were modeled as oxygen atoms. Accordingly, the exact formula was determined by elemental analyses. A summary of the crystallographic data and structure refinement for compounds **1** and **2** is given in Table 1. Complete crystallographic details are included in the Supporting Information.

Results and Discussion

Crystal Structures of $[Fe_2(AsMo_7O_{27})_2]^{12-}$ (1a) and $[FeCr(AsMo_7O_{27})_2]^{12-}$ (2a). The two polyanions, $[Fe_2(AsMo_7O_{27})_2]^{12-}$ (**1a**) and $[FeCr(AsMo_7O_{27})_2]^{12-}$ (**2a**), are isomorphous and consist of two $[AsMo_7O_{27}]^{9-}$ moieties linked via a $[MM'O_{10}]$ (MM′ = FeFe, CrFe) group, leading to a sandwich-type structure (see Figure 1). This structural type was described previously by us for $[Cr_2(AsMo_7O_{27})_2]^{12-}$ and $[Cu_2(AsMo_7O_{27})_2]^{14-}$.[15] However, the title polyanions represent the first example of iron-sandwiched and mixed-metal-sandwiched polymolybdates. The $[AsMo_7O_{27}]$ fragment contains an AsO_3 triangular pyramid and seven edge-sharing MoO_6 octahedra, and it can be considered as a monocapped hexavacant α-B-Keggin subunit with a central AsO_3 group and can be derived from the well-known trivacant Keggin ion, α-B-$As^{III}Mo_9O_{33}^{9-}$, by moving one Mo_3O_{13} unit from the α-B-$AsMo_9O_{33}$ unit and inserting one MoO_6 octahedron in the hole between the two residual Mo_3O_{13} units. The structure of the fragment is very similar to that of the bridging fragment $[CoW_7O_{26}(OH)_2]$ in the double-sandwich polyanion $[Co_7(H_2O)_2(OH)_2P_2W_{25}O_{94}]^{16-}$,[20] except that the CoO_4 tetrahedron was replaced by an AsO_3 triangular pyramid. Assuming that the two metallic positions are crystallographically equivalent (M = 1/2Cr + 1/2Fe) for **2a**, the polyanion displays C_{2h} molecular symmetry with a C_2 axis along two center ions as its Fe analogue. Each metal cation presents a distorted octahedral environment comprising two μ_3-O(AsMM′) bridging oxygen atoms and four μ_2-O_t(MoM) atoms of the $AsMo_7O_{27}$ groups. And the two central transition metal ions (MM′) are bridged by two μ_3-O(AsMM′) atoms. Selected bond distances and angles for $[Fe_2(AsMo_7O_{27})_2]^{12-}$ (**1a**), $[FeCr(AsMo_7O_{27})_2]^{12-}$ (**2a**), and $[Cr_2(AsMo_7O_{27})_2]^{12-}$ (**3a**) are compared in Table 2. As expected, the M−O, M···M′, and As···As′ distances get shorter in the order of $[Fe_2(AsMo_7O_{27})_2]^{12-}$, $[FeCr(AsMo_7O_{27})_2]^{12-}$, and $[Cr_2(AsMo_7O_{27})_2]^{12-}$. This observation is in complete agreement with the size difference between the Fe^{3+}(r = 0.645 Å) and Cr^{3+} (r = 0.615 Å). The distances of two transition metals in **1a**−**3a** are 3.119(6) Å (Fe···Fe), 3.087(6) Å (Cr···Fe), and 3.049(7) Å (Cr···Cr), respectively, which are much smaller than the 5 Å of the corresponding oxalato-bridged dinuclear complexes.[16]

Synthesis. Reaction of a solution of As_2O_3 with $(NH_4)_6Mo_7O_{24}\cdot 4H_2O$, Fe^{3+}, or Cr^{3+}, or a mixture of Fe^{3+} and Cr^{3+} at 90 °C and in a pH = 6.5−7.0 aqueous solution allowed us to obtain the homometallic sandwich arsenatomolybdates, $(NH_4)_{12}[Fe_2(AsMo_7O_{27})_2]\cdot 12H_2O$ (**1**) or $(NH_4)_{12}[Cr_2(AsMo_7O_{27})_2]\cdot 11H_2O$ (**3**), or the heterometallic Cr(III)−Fe(III) sandwich arsenatomolybdate, $(NH_4)_{12}[FeCr(AsMo_7O_{27})_2]\cdot 13H_2O$ (**2**), in about 85% yield. In the process of synthesis, the pH value is a crucial factor affecting the isolation of title compounds and should carefully be maintained at 6.5−7.0. When the

(20) Clemente-Juan, J. M.; Coronado, E.; Forment-Aliaga, A.; Galán-Mascarós, J. R.; Giménez-Saiz, C.; Gómez-García, C. J. *Inorg. Chem.* **2004**, *43*, 2689.

Table 2. Selected Bond Distances (Å) and Angles (deg) for $[Fe_2(AsMo_7O_{27})_2]^{12-}$ (**1a**), $[FeCr(AsMo_7O_{27})_2]^{12-}$ (**2a**), and $[Cr_2(AsMo_7O_{27})_2]^{12-}$ (**3a**)

	1a	2a	3a[15]
M−(μ_3-O)	2.019(6), 2.036(6)	2.006(6), 2.019(6)	1.993(7)−1.998(7)
M−(μ_2-O)	1.962(7)−2.008(6)	1.949(6)−1.983(6)	1.938(7)−1.965(7)
As···As′	6.088(6)	6.073(6)	6.058(7)
M···M′	3.119(6)	3.087(6)	3.049(7)
M−(μ_3-O)−M	100.6(3)	100.0(3)	99.6(3)
(μ_2-O)−M−(μ_2-O)	89.7(3)−95.5(3)	89.8(3)−94.9(3)	88.9(3)−95.2(3)
(μ_3-O)−M−(μ_3-O)	79.4(3)	79.8(3)	80.4(3)

pH was higher than 7, there was an abundance of precipitation, and when the pH was lower than 6.5, we could not isolated the title compounds. The stability of compounds **1** and **2** in water has been studied using the time-dependent UV−vis spectra of a 2 mM aqueous solution (pH = 6.5). The spectrum of a fresh sample (taken within seconds after dissolving the complexes in water) shows an absorption band below ca. 470 nm, and with the extension of time, the profile of the spectra changes with a decrease in intensity (Figure S1, Supporting Information). Within several minutes, the hydrolytic decomposition seems to be complete, and the spectrum does not undergo any further changes. The results may mean that the compounds are unstable in the aqueous solution.

Thermal Analyses. According to the TG-DSC curve of compound **1** (Figure S2, Supporting Information), we can deduce that the thermal decomposition process of the compound is approximately divided into three steps. There is a continuous decrease in the range 30−286 °C, and a weight loss of 14.6% is comparable with the calculated value of 14.9%, corresponding to the loss of all water and NH_3 molecules. The second weight loss of 6.2% (calcd 6.8%) is between 286 and 409 °C, accompanying a remarkable exothermal peak at 375 °C in the DSC curve due to the escaping of As_2O_3. The third stage is the decomposition of the Mo−Fe−O framework structure accompanying an exothermal peak at 445 °C in the DSC curve. The final product should be the mixed-metal oxide $Fe_2Mo_{14}O_{45}$, and the observed total weight loss of 25.5% compares well with the calculated value of 25.0%.

The TG curve of compound **2** (Figure S3, Supporting Information) is similar with that of compound **1**. First, it gradually loses all water and NH_3 molecules in the range 30−283 °C. The total weight loss of 15.1% is consistent with the calculated value of 15.4%. Then, a weight loss of 7.5% (calcd 6.8%) from 283 to 410 °C is ascribed to the escaping of As_2O_3. The last stage is the decomposition of the Mo−Fe−Cr−O framework structure, and the final product should be the mixed-metal oxide $FeCrMo_{14}O_{45}$. The observed total weight loss of 25.8% compares well with the calculated value of 25.5%.

Magnetic Susceptibility. The variable-temperature magnetic susceptibility (χ_M) of compounds **1**, **2**, and **3** was examined in a 1000 Oe field in the 2.0−300.0 K. The $\chi_M T$ versus T plots are shown in Figure 2. At 300 K, the $\chi_M T$ values are 8.89, 6.27, and 3.33 cm^3 K mol^{-1} for compounds **1**−**3**, respectively, corresponding to the calculated spin-only value 8.75, 6.25, and 3.75 cm^3 K mol^{-1} for Fe^{III} (S = 5/2) and Cr^{III} (S = 3/2) with $g_{Fe} = g_{Cr} = 2$. Upon cooling, the $\chi_M T$ values decline monotonously and reach 0.14, 1.00, and 0.11 cm^3 K mol^{-1} at 2.0 K for **1**, **2**, and **3**, respectively, indicating a significant antiferromagnetic exchange between the magnetic centers in compounds **1**−**3**. The $\chi_M T$ value of compound **2** reaches 1.00 cm^3 K mol^{-1} down to 2.0 K, corresponding to the low-temperature limit (Figure S4, Supporting Information):

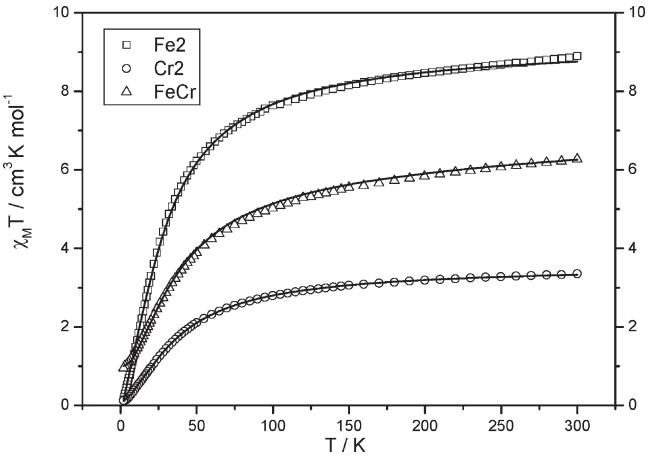

Figure 2. Plots of $\chi_M T$ (cm^3 mol^{-1} K) versus T (K) for compounds **1** (□), **2** (Δ), and **3** (○). The solid lines represent the fit to the appropriate theoretical equation.

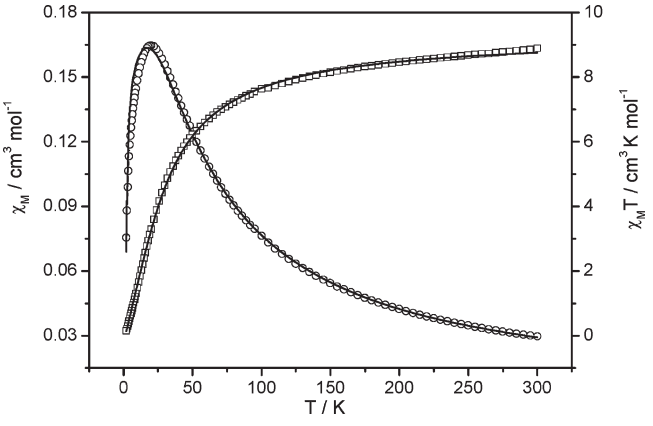

Figure 3. Plots of χ_M and $\chi_M T$ versus T for compound **1**. Experimental data, circles and squares; best theoretical fit, solid lines.

$$(\chi_M T)_{LT} = \frac{N g_s^2 \beta^2}{3k}[(S_{Fe} - S_{Cr})^2 + |S_{Fe} - S_{Cr}|]^{19}$$

The χ_M value for **1** increases continuously on cooling from room temperature until approaching a maximum of 0.1636 cm^3 mol^{-1} at 17 K (Figure 3). Then, it decreases quickly to a value of 0.0755 cm^3 mol^{-1} down to 2 K. The maximum appearing in the χ_M versus T curve indicates a significant antiferromagnetic couple between two Fe^{3+} ions through two μ-O bridges. Similar antiferromagnetic exchange coupling is also observed in compound **3** between two Cr^{3+} ions. The maximum 0.0488 cm^3 mol^{-1} appears at 22 K in the χ_M versus T curve (Figure 4). Then, it decreases, reaching a minimum of 0.0347 cm^3 mol^{-1} at 4 K, different from compound **1**, below which the χ_M of

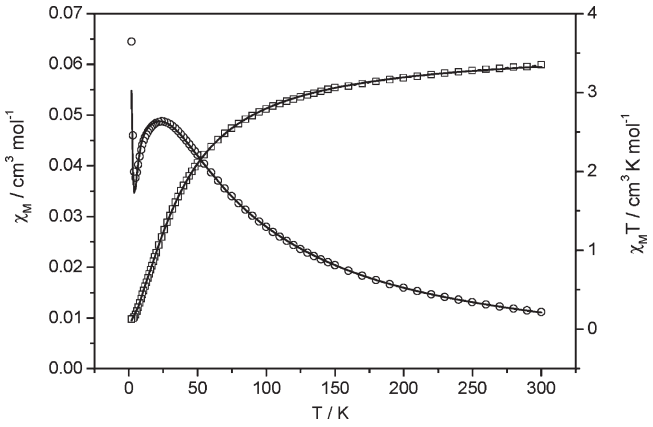

Figure 4. Plots of χ_M and $\chi_M T$ versus T for compound **3**. Experimental data, circles and squares; best theoretical fit, solid lines.

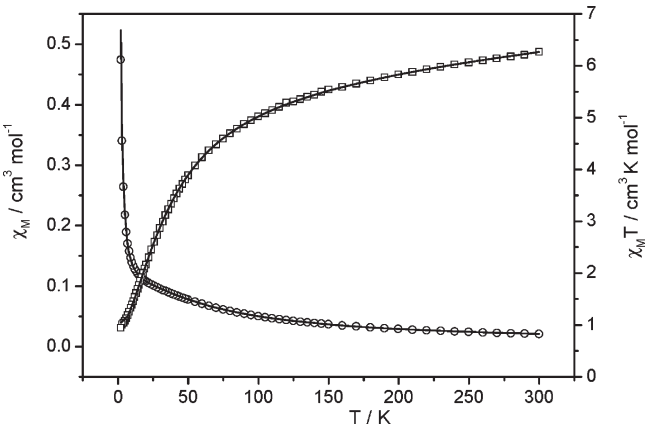

Figure 5. Plots of χ_M and $\chi_M T$ versus T for compound **2**. Experimental data, circles and squares; best theoretical fit, solid lines.

compound **3** increases again. This behavior is typical for an antiferromagnetically coupled system with the presence of a small amount of paramagnetic impurities.

The magnetic data of compounds **1** and **3** were fitted using a model which considers the Hamiltonian $H = -2JS_1S_2$. Terms corresponding to the intermolecular interaction zJ' and a paramagnetic impurity ρ were also included. The final expression is

$$\chi = \frac{\chi'}{1-(2zJ'/Ng^2\beta^2)\chi'}$$

$$\chi' = (1-\rho)\chi_{M_2} + \rho\frac{2Ng^2\beta^2}{3kT}S_M(S_M+1) \quad (M = Fe \text{ or } Cr)$$

$$\chi_{Fe_2} = \frac{2Ng^2\beta^2}{kT} \times \frac{55e^{30J/kT} + 30e^{20J/kT} + 14e^{12J/kT} + 5e^{6J/kT} + e^{2J/kT}}{11e^{30J/kT} + 9e^{20J/kT} + 7e^{12J/kT} + 5e^{6J/kT} + 3e^{2J/kT} + 1}$$

$$\chi_{Cr_2} = \frac{2Ng^2\beta^2}{kT} \times \frac{e^{2J/kT} + 5e^{6J/kT} + 14e^{12J/kT}}{1 + 3e^{2J/kT} + 5e^{6J/kT} + 7e^{12J/kT}}$$

The best fits, shown as solid lines in Figures 3 and 4, led to parameters $g = 2.06$ (0.002), $J = -2.09$ (0.03) cm^{-1}, $zJ' = -0.01$ (0.004) cm^{-1}, $\rho = 0.1\%$ (0.06%) (least-squares analysis $R = 3.7 \times 10^{-3}$) for compound **1** and $g = 1.96$ (0.001), $J = -6.26$ (0.05) cm^{-1}, $zJ' = -0.02$ (0.007) cm^{-1}, $\rho = 3\%$ (0.1%) ($R = 8 \times 10^{-5}$) for compound **3**, respectively.

For compound **2**, which is an FeCr heterodinuclear with different $S_{Fe} = 5/2$ and $S_{Cr} = 3/2$ local spins, the continuous increasing of χ_M upon cooling is mainly due to the paramagnetic ground state $S = 1$ (Figure 5). The susceptibility data were fitted using the Wigner−Eckart theorem.[19]

$$g_S = \frac{1+c}{2}g_{Fe} + \frac{1-c}{2}g_{Cr} \text{ with } c = \frac{S_{Fe}(S_{Fe}+1) - S_{Cr}(S_{Cr}+1)}{S(S+1)}$$

The final expression of this model is

$$g_1 = \frac{-3g_{Cr} + 7g_{Fe}}{4}, g_2 = \frac{g_{Cr} + 11g_{Fe}}{12}, g_3 = \frac{7g_{Cr} + 17g_{Fe}}{24}, g_4 = \frac{3g_{Cr} + 5g_{Fe}}{8}$$

$$\chi_{FeCr} = \frac{2N\beta^2}{3kT} \times \frac{3g_1^2 + 15g_2^2e^{4J/kT} + 42g_3^2e^{10J/kT} + 90g_4^2e^{18J/kT}}{3 + 5e^{4J/kT} + 7e^{10J/kT} + 9e^{18J/kT}} + \text{TIP}$$

The best fits, shown as solid lines in Figure 5, resulted in parameters $g_{Cr} = 1.88$ (0.005), $g_{Fe} = 1.97$ (0.003), $J = -3.9$ (0.02) cm^{-1}, and TIP = 245 (0.3) $\times 10^{-6}$ ($R = 3.3 \times 10^{-4}$) for compound **2**. Fixed $g_{Fe} = g_{Cr} = 2.0$, the fit, shown as the solid line in Figure S5 (Supporting Information), gave parameters $J = -4.1$ cm^{-1} and TIP = 118 $\times 10^{-6}$ ($R = 2.8 \times 10^{-3}$).

It is well-known that the magnetic coupling depends on the nature and structure of magnetic ions and bridging ligands, and it can be influenced by the M−O−M′ angle as well as the M···M′ distance. When the angle is close to 180°, the strongest antiferromagnetic interaction would be found in the compound. With decreasing M−O−M′ angle and increasing M···M′ distance, the antiferromagnetic exchange decreases. In compounds **1**, **2**, and **3**, two central transition metal ions (MM′) are bridged by two μ-O atoms. M−O−M′ angles, ranging from 99.6° to 100.6° (Table 2), are very close to 97.5°. A weak antiferromagnetic exchange between the magnetic centers in compounds **1**−**3** would be expected through the μ-O bridges. Indeed, the magnetic coupling J values calculated for **1**, **2**, and **3** are −2.09, −4.09, and −6.26 cm^{-1}, respectively. Compared with the values of −3.84, 1.10, and −3.23 m^{-1} for the corresponding oxalato-bridged dinuclear complexes $[(C_2H_5)_4N]_4[MM'(ox)(NCS)_8]$ (MM′ = FeFe, CrFe, and CrCr),[16a] the main difference is that the heterometallic oxalato-bridged dinuclear compound is ferromagnetic but weak antiferromagnetic for $(NH_4)_{12}[FeCr(AsMo_7O_{27})_2]\cdot 13H_2O$ (**2**). So far, rather few

(21) Sadun, C.; Bucci, R.; Magrì, A. L. *J. Am. Chem. Soc.* **2002**, *124*, 3036.

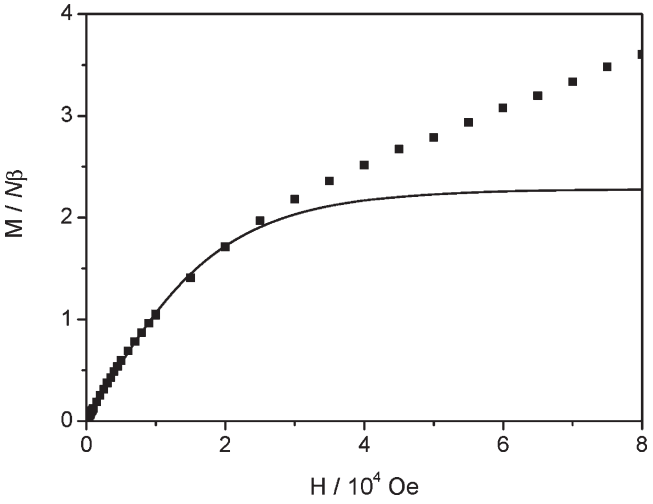

Figure 6. Magnetization vs magnetic field curve at 2.0 K for compound **2**. Experimental data, full circles; the fit to a Brillouin function for an $S = 1$ spin state below 20 kOe with an effective g value of 2.28, solid lines.

magnetic studies on two μ-O bridged heterobinuclear FeO_2Cr compounds have been reported.[21] The magnetic investigations have been centered on the family of one μ-O bridged heterodinuclear FeOCr complexes with the formula (L)FeOCr(L′).[17] Consequently, compound $[(TPA)(OH)FeOFe(OH)(TPA)]^{2+}$ (TPA = tris(2-pyridylmethyl)-amine) with an Fe−O−Fe angle of 158° has a J value of -115 cm^{-1}.[17a] Magnetic susceptibility measurements without structure determination on a series of heterodinuclear $Fe^{3+}OCr^{3+}$ complexes, (TPP)FeOCr(L) [tpp = dianion of 5,10,15,20-tetra phenylporphyrin; L = dianion of N,N′-(4-methyl-4-azaheptane-1,7-diyl)bis(salicyli-deneimine), other tetradentate salicylideneimines, or anions of dithiocarbamates], resulted in J values in the range -130 to -150 cm^{-1}.[17b] In addition, spin exchange coupling in the asymmetric heterodinuclear complexes containing the μ-oxo-bis(μ-acetato) dimetal core, [L′Cr(μ−OH)(μ-CH_3CO_2)$_2$FeL]$(PF_6)_2$,[22a] [L′Cr(μ-O)(μ-CH_3CO_2)$_2$FeL]$(C1O_4)_2 \cdot H_2O$, and [L′Cr(μ−OH)(μ-CH_3CO_2)$_2$FeL]$(C1O_4)_3 \cdot 2H_2O$[22b] (L = 1,4,7-triazacyclononane, L′ = 1,4,7-trimethyl-1,4,7-triazacyclononane) with J values of -137, -275, and -43 cm^{-1}, respectively, has been reported.

The magnetization M versus H curve for compound **2** at 2.0 K is shown in Figure 6. It is close to a Brillouin function with ground state $S = 1$ up to 20 kOe, resulting in an effective g value of 2.28. But, instead of showing a saturation magnetization $M = gN\beta$ above 20 kOe, M continuously increases and reaches 3.6 $N\beta$ at 80 kOe. This behavior can be explained as follows: when H increases, the gaps between the ground state and the other excited states decrease. The magnetization increase could be due to the level crossing of different spin states induced by the high external field, and the effect of impurities cannot be excluded either.[23]

In conclusion, we have simultaneously synthesized the homometallic sandwich POMs $(NH_4)_{12}[Fe_2(AsMo_7O_{27})_2] \cdot 12H_2O$ and $(NH_4)_{12}[Cr_2(AsMo_7O_{27})_2] \cdot 11H_2O$ and the first example of the "symmetrical" heterometallic Cr(III)−Fe(III) sandwich POM, $(NH_4)_{12}[As_2FeCrMo_{14}O_{54}] \cdot 13H_2O$. Their magnetic properties are investigated thoroughly. The magnetic results clearly establish that compound **2** is formed by bimetallic Cr(III)−Fe(III) units and not by a mixture of the two antiferromagnetically coupled homometallic species. This work further proves that the novel fragment $[AsMo_7O_{27}]$ is a basic building unit used to construct the more homometallic and heterometallic sandwich POMs, and the more complicated arsenomolybdates with more interesting properties based on fragment $[AsMo_7O_{27}]$ could be expected.

Acknowledgment. This work was supported by the National Natural Science Foundation of China (20973133), the Education Commission of Shaanxi Province (09JK783), Funded Projects of Independent Innovation of Northwest University Postgraduates (08YZZ41), and Talented People Science Foundation of Northwest University (PR08045).

Supporting Information Available: The crystallographic information files (CIF) for $(NH_4)_{12}[Fe_2(AsMo_7O_{27})_2] \cdot 12H_2O$ (**1**) and $(NH_4)_{12}[FeCr(AsMo_7O_{27})_2] \cdot 13H_2O$ (**2**); time profile of the electronic absorption spectra of a 2 mM aqueous solution (pH = 6.5) of $(NH_4)_{12}[Fe_2(AsMo_7O_{27})_2] \cdot 12H_2O$ (**a**) and $(NH_4)_{12}[FeCr(AsMo_7O_{27})_2] \cdot 13H_2O$ (**b**) (Figure S1); TG-DSC curves of compound **1** (Figure S2−S3); plot of the $\chi_M T$ (cm^3 mol^{-1} K) of complexes **1**−**3** in 2.0−25 K (Figure S4); the χ_M and $\chi_M T$ plots for compound **2** (Figure S5). These materials are available free of charge via the Internet at http://pubs.acs.org.

(22) (a) Slep, L. D.; Mijovilovich, A.; Meyer-Klaucke, W.; Weyhermüller, T.; Bill, E.; Bothe, E.; Neese, F.; Wieghardt, K. *J. Am. Chem. Soc.* **2003**, *125*, 15554. (b) Hotzelmann, R.; Wieghardt, K.; Flörke, U.; Haupt, H.-J.; Weatherburn, D. C.; Bonvoisin, J.; Blondin, G.; Girerd, J.-J. *J. Am. Chem. Soc.* **1992**, *114*, 1681.

(23) Ménage, S.; Vitols, S. E.; Bergerat, P.; Codjovi, E.; Kahn, O.; Girerd, J.-J.; Guillot, M.; Solans, X.; Calvet, T. *Inorg. Chem.* **1991**, *30*, 2666.